Published in final edited form as:
*Conf Proc IEEE Eng Med Biol Soc*. 2011 ; 2011: 3732–3735. doi:10.1109/IEMBS.2011.6090635.

# Four-Dimensional MR Cardiovascular Imaging: Method and Applications

**Anthony G. Christodoulou**,
Department of Electrical and Computer Engineering and Beckman Institute for Advanced Science and Technology, University of Illinois at Urbana-Champaign, 1406 West Green Street, Urbana, IL 61801

**Bo Zhao**,
Department of Electrical and Computer Engineering and Beckman Institute for Advanced Science and Technology, University of Illinois at Urbana-Champaign, 1406 West Green Street, Urbana, IL 61801

**Haosen Zhang**,
Pittsburgh NMR Center for Biomedical Research, Department of Biological Sciences, Carnegie Mellon University, 4400 Fifth Avenue, Pittsburgh, PA 15213

**Chien Ho**, and
Pittsburgh NMR Center for Biomedical Research, Department of Biological Sciences, Carnegie Mellon University, 4400 Fifth Avenue, Pittsburgh, PA 15213

**Zhi-Pei Liang**
Department of Electrical and Computer Engineering and Beckman Institute for Advanced Science and Technology, University of Illinois at Urbana-Champaign, 1406 West Green Street, Urbana, IL 61801

Anthony G. Christodoulou: christo8@illinois.edu

## Abstract

Magnetic resonance imaging (MRI) has long been recognized as a powerful tool for cardiovascular imaging because of its unique potential to measure blood flow, cardiac wall motion and tissue properties jointly. However, many clinical applications of cardiac MRI have been limited by low imaging speed. Three-dimensional cardiovascular MRI in real-time, or 4D cardiovascular MRI without cardiac and respiratory gating or triggering, remains an important technological goal of the MR cardiovascular research community. In this paper, we present a novel technique to achieve 4D cardiovascular MR imaging in unprecedented spatiotemporal resolution. This breakthrough is made possible through a creative use of sparse sampling theory and parallel imaging with phased array coils and a novel implementation of data acquisition and image reconstruction. We have successfully used the technique to perform 4D cardiovascular imaging on rats, achieving 0.65 mm × 0.65 mm × 0.31 mm spatial resolution with a frame rate of 67 fps. This capability enables simultaneous imaging of cardiac motion, respiratory motion, and first-pass myocardial perfusion. This in turn allows multiple cardiac assessments including measurement of ejection fraction, cardiac output, and myocardial blood flow in a single experiment. We believe that the proposed technique can open up many important applications of cardiovascular imaging and have significant impact on the field.



Correspondence to: Anthony G. Christodoulou, christo8@illinois.edu.

# I. INTRODUCTION

Cardiovascular diseases such as congenital heart disease or coronary artery disease are a major cause of death around the globe. It has long been a dream of imaging scientists to develop advanced imaging methods capable of capturing the structural and functional changes of the beating heart in real time. Over the last five decades, significant progress has been made, leading to the successful development and application of several noninvasive cardiac imaging modalities, including echocardiography [1], cardiac CT [2], cardiac PET (positron emission tomography) [3], cardiac SPECT (single photon emission computed tomography) [4], and cardiac MRI (magnetic resonance imaging) [5]. While these modalities have complementary strengths and applications, cardiovascular MR (CMR) has been a key research focus for the last two decades because of its unique potential to allow multiple comprehensive cardiac assessments in a single integrated examination [6], such as measurement of blood flow and cardiac wall motion, assessment of tissue properties, etc. [7]. Through these dedicated efforts of researchers in academia and industry, CMR has become the clinical gold standard for several cardiovascular assessments [8]. However, the limited imaging speed of existing MR technology is still a major technical barrier which has prevented practical application of CMR for comprehensive examination of the heart.

There are three key approaches to accelerating the MR imaging process: a) fast scanning using special pulse sequences, b) parallel imaging using phased array coils, and c) sparse sampling. In this paper, we present a novel cardiac imaging method that synergistically integrates all three of these approaches. We have successfully used the technique to perform 4D cardiovascular imaging on rats, achieving 0.65 mm × 0.65 mm × 0.31 mm spatial resolution with a frame rate of 67 fps. This unprecedented capability enables simultaneous imaging of cardiac motion, respiratory motion, and first-pass myocardial perfusion. This in turn allows multiple cardiac assessments including measurement of ejection fraction, cardiac output, and myocardial blood flow in a single experiment. We believe that the proposed technique can open up many important applications of cardiovascular imaging and have significant impact on the field.

The rest of the paper is organized as follows: Section II describes the proposed method in detail; Section III shows some representative 4D CMR experimental results obtained using the proposed method, and Section IV contains the conclusion of the paper.

# II. THE PROPOSED METHOD

The proposed method achieves high-speed cardiac imaging by using a novel data acquisition scheme that sparsely samples (**k**, $t$)-space. The sparse sampling scheme is enabled by a new image reconstruction algorithm capable of reconstructing high-quality images from highly undersampled data. In this section, we describe our proposed method in detail.

## A. High-speed data acquisition with sparse sampling of (k, *t*)-space

Acceleration of data acquisition in the proposed imaging method is achieved by sampling (**k**, $t$)-space well below the Nyquist rate. Specifically, we effectively integrate: a) sparse sampling based on compressed sensing (CS), b) sparse sampling based on partial separability (PS), and c) sparse sampling based on sensitivity encoding using phased array coils (often known as parallel imaging).

More specifically, let $\rho(\mathbf{r}, t)$ be the desired spatiotemporal image function representing the structural and functional changes of the heart. The data acquired using an array of $P$ coils can be expressed as

$$d_p(\mathbf{k}, t) = \int S_p(\mathbf{r}) \rho(\mathbf{r}, t) e^{-i2\pi \mathbf{k}\cdot\mathbf{r}} d\mathbf{r}, \quad (1)$$

where $S_p(\mathbf{r})$ is the sensitivity encoding function of the $p$th coil. According to multichannel sampling theory [9], we can undersample $d_p(\mathbf{k}, t)$ up to a factor of $P$ below the Nyquist rate. However, a much smaller downsampling factor is achieved in practice due to the well-known ill-conditoning problem associated with parallel imaging using phased array coils [9]. In our proposed method, we achieve another factor of undersampling by exploiting two key mathematical properties of $(\mathbf{k}, t)$-space signals: a) spatial-spectral sparsity, and b) partial separability.

The use of signal sparsity for sparse sampling is the core of the celebrated compressed sensing theory [10]–[12] which has recently found useful applications in MRI [13], [14]. For cardiac imaging, it is reasonable to assume that $\mathcal{F}_t\{\rho(\mathbf{r}, t)\}$ is sparse (or highly compressible) [15], as shown in Fig. 1. Based on compressed sensing theory, we can recover $\rho(\mathbf{r}, t)$ from undersampled $(\mathbf{k}, t)$-space signals by solving the following convex optimization problem:

$$\arg\min_{\rho(\mathbf{r},t)} \sum_{p=1}^{P} \| d_p(\mathbf{k}_m, t_n) - \int S_p(\mathbf{r}) \rho(\mathbf{r}, t_n) e^{-i2\pi \mathbf{k}_m\cdot\mathbf{r}} d\mathbf{r} \|_2^2 + \lambda \left\| \mathcal{F}_t\{\rho(\mathbf{r}, t)\} \right\|_1. \quad (2)$$

In our proposed method, we further accelerate the data acquisition by taking advantage of the fact that the $(\mathbf{k}, t)$-space cardiac signals are partially separable. More specifically, we express $d_p(\mathbf{k}, t)$ as

$$d_p(\mathbf{k}, t) = \sum_{\ell=1}^{L} \alpha_{p,\ell}(\mathbf{k}) \varphi_\ell(t), \quad (3)$$

which is called $L$th-order partially separable [16]. Note that the temporal basis $\{\varphi_\ell(t)\}_{\ell=1}^{L}$ is independent of the coil under the assumption that the coil sensitivity function $S_p$ is time-invariant. The property of $L$th-order partial separability implies that the following Casorati matrix

$$\mathbf{C} = \begin{bmatrix} d_p(\mathbf{k}_1, t_1) & d_p(\mathbf{k}_1, t_2) & \dots & d_p(\mathbf{k}_1, t_N) \\ d_p(\mathbf{k}_2, t_1) & d_p(\mathbf{k}_2, t_2) & \dots & d_p(\mathbf{k}_2, t_N) \\ \vdots & \vdots & \ddots & \vdots \\ d_p(\mathbf{k}_M, t_1) & d_p(\mathbf{k}_M, t_2) & \dots & d_p(\mathbf{k}_M, t_N) \end{bmatrix}$$

has at most rank $L$. Cardiac $(\mathbf{k}, t)$-space signals are often partially separable to a low order (as illustrated in Fig. 2) because the high degree of spatiotemporal correlation makes $\{d_p(\mathbf{k}_m, t)\}_{m=1}^{M}$ linearly dependent ($M > L$).

Sparse sampling of $(\mathbf{k}, t)$-space results in many missing entries in $\mathbf{C}$. It has been shown that $\mathbf{C}$ can be recovered by imposing rank constraints [17], [18], specifically by solving the following optimization problem:

$$\arg \min_{\widehat{\mathbf{C}} \in \mathbb{C}^{M \times N}} \operatorname{rank}(\widehat{\mathbf{C}}) \quad \text{s.t.} \quad \left\| \Omega(\widehat{\mathbf{C}}) - \Omega(\mathbf{C}) \right\|_2^2 < \delta,$$

where $\mathbf{C}$ is the data matrix with missing entries as specified by the sparse sampling operator $\Omega$, $\hat{\mathbf{C}}$ is the recovered matrix, and $\delta$ specifies some allowable data discrepancy.

An important novelty of the proposed method is the effective integration of the above sparse sampling strategies for high-speed cardiac imaging, which is further enabled by a novel image reconstruction method to be described in the following subsection. The proposed data acquisition method can be implemented in a number of ways. One strategy is to sample ($\mathbf{k}$, $t$)-space in a fashion yielding two data sets, one with high temporal resolution at limited $\mathbf{k}$-space locations, and the other covering the "full" $\mathbf{k}$-space (to provide the desired spatial resolution) but with very low temporal resolution. An example of this sampling strategy is illustrated in Fig. 3. This data acquisition strategy can significantly simplify the underlying image reconstruction problem.

### B. Image reconstruction from highly undersampled data

High-quality image reconstruction from highly undersampled ($\mathbf{k}$, $t$)-space data is made possible in the proposed method through the use of three constraints: a) a partial separability constraint, b) a spatial-spectral sparsity constraint, and c) a data consistency constraint. Based on the PS model in Eq. (3), the desired image function can be expressed as

$$\rho(\mathbf{r}, t) = \sum_{\ell=1}^{L} \psi_\ell(\mathbf{r}) \varphi_\ell(t), \tag{4}$$

Using the data acquisition strategy described in the previous subsection, we can first use the high temporal resolution data to determine the temporal basis functions $\{\widehat{\varphi}_\ell(t)\}_{\ell=1}^{L}$ through subspace estimation techniques such as singular value decomposition. The spatial coefficients $\{\psi_\ell(\mathbf{r})\}_{\ell=1}^{L}$ are then determined by solving the following optimization problem:

$$\arg \min_{\{\psi_\ell(\mathbf{r})\}_{\ell=1}^{L}} \sum_{p=1}^{P} D_p(\{\psi_\ell(\mathbf{r})\}_{\ell=1}^{L}) + \lambda \left\| \mathcal{F}_t \left\{ \sum_{\ell=1}^{L} \psi_\ell(\mathbf{r}) \widehat{\varphi}_\ell(t) \right\} \right\|_1, \tag{5}$$

where $D_p(\{\psi_\ell(\mathbf{r})\}_{\ell=1}^{L})$ is a measure of the consistency between the reconstructed image and the measured data $\{d_p(\mathbf{k}_m, t_n)\}_{m,n=1}^{M,N}$ from the $p$th receiver coil,

$$D_p(\{\psi_\ell(\mathbf{r})\}_{\ell=1}^{L}) = \left\| d_p(\mathbf{k}_m, t_n) - \sum_{\ell=1}^{L} \int S_p(\mathbf{r}) \psi_\ell(\mathbf{r}) \widehat{\varphi}_\ell(t_n) e^{-i2\pi \mathbf{k}_m \cdot \mathbf{r}} d\mathbf{r} \right\|_2^2.$$

The resulting optimization problem is convex, and can be solved using a number of optimization algorithms. Here, we solve the problem by combining an additive half-quadratic optimization algorithm with a continuation procedure [19].

## III. APPLICATIONS AND RESULTS

The proposed method opens up a range of possibilities to image the structure and function of the beating heart. In addition to providing a new capability to perform multiple integrated cardiac assessments in a single imaging experiment, high-resolution 4D CMR can significantly increase the accuracy and utility of many cardiac assessments, including measurements of ejection fraction, cardiac output, and myocardial perfusion. In this paper, we demonstrate its capability to image cardiac motion and contrast-enhanced first-pass myocardial perfusion simultaneously.

First-pass myocardial perfusion imaging is most commonly performed using ECG-triggered multislice 2D imaging, wherein different slices correspond to different cardiac phases. Unfortunately, not all cardiac phases are equally useful or simple to image: although myocardial signal intensity as normalized by left ventricular blood pool signal intensity is generally considered independent of the cardiac phase, the end-systolic phase has maximal myocardial thickness, making it easier to distinguish separate layers of the myocardium [20]. Our proposed method avoids the problem of phase-unmatched slices, as phase-matched 3D images from arbitrary cardiac phases are easily extracted from 4D images.

We have implemented our technique on a Bruker (Billerica, MA) Avance AV1 4.7 T, 40 cm equipped with a 12 cm, 40 G/cm shielded gradient set and a 4-channel array coil. A customized FLASH pulse sequence with $T_R$ = 7.5 ms and $T_E$ = 2.4 ms was used to acquire data at 62 × 62 × 128 matrix size over a 4 cm × 4 cm × 4 cm FOV for an effective spatial resolution of 0.65 mm × 0.65 mm × 0.31 mm. The reconstructions have a frame rate of 67 fps.

Data were collected continuously with neither gating nor breath holding, using the data acquisition strategy previously described. Dynamic contrast enhancement for first-pass myocardial perfusion imaging was performed by injecting a 0.2 mmol/kg bolus of gadolinium contrast agent (Gd-DTPA) into each subject after the start of data acquisition.

The animals used in the study were Dark-Agouti and Brown Norway rats as in [21]. All animals received humane care in compliance with the *Guide for the Care and Use of Laboratory Animals*, published by the National Institutes of Health, and the animal protocol was approved by the Carnegie Mellon University Institutional Animal Care and Use Committee.

Figure 4 depicts cardiovascular structure over a single respiratory cycle. Both cardiac motion and respiratory motion are visible in the reconstruction. The structural information in this figure enables measurement of ejection fraction, cardiac output, and other cardiac assessments. The images in Fig. 5 depict the wash-in of Gd-DTPA during the same experiment. This figure also includes a representative signal intensity curve taken from one region of the myocardium. In order to better illustrate dynamic contrast enhancement, the image contrast window of Fig. 5 is wider than that of Fig. 4.

## IV. CONCLUSIONS

This paper presents a novel method for whole-heart 4D cardiovascular magnetic resonance imaging integrating parallel imaging, fast-scanning, and sparse sampling. The proposed method enables 4D imaging of *in vivo* rat hearts at 0.65 mm × 0.65 mm × 0.31 mm spatial resolution and a frame rate of 67 fps. We have presented the first demonstration of 4D CMR capable of imaging cardiac motion, respiratory motion, and dynamic contrast enhancement in a single experiment. The proposed method can have far-reaching implications for diagnosis and assessment of cardiovascular diseases.

## Acknowledgments

The work was supported in part by NIH-P41-EB001977, NIH-P41-RR023953, NSF-CBET-07-30623, and a predoctoral fellowship (AGC) from the American Heart Association.

## References

1. Lindström K, Edler I. The history of echocardiography. Ultrasound Med Biol. Dec; 2004 30(12): 1565–1644. [PubMed: 15617829]
2. Roberts WT, Bax JJ, Davies LC. Cardiac CT and CT coronary angiography: Technology and application. Heart. Jun; 2008 94(6):781–792. [PubMed: 18480352]
3. Bengel FM, Higuchi T, Javadi MS, Lautamäki R. Cardiac positron emission tomography. J Am Coll Cardiol. Jun; 2009 54(1):1–15. [PubMed: 19555834]
4. DePuey, EG.; Garcia, EV.; Berman, DS. Cardiac SPECT imaging. 2. Philadelphia, PA: Lippincott Williams & Wilkins; 2001.
5. Finn JP, Nael K, Deshpande V, Ratib O, Laub G. Cardiac MR imaging: State of the technology. Radiology. Nov; 2006 241(2):338–354. [PubMed: 17057063]
6. Schalla S, Nagel E, Lehmkuhl H, Klein C, Bornstedt A, Schnackenburg B, Schneider U, Fleck E. Comparison of magnetic resonance real-time imaging of left ventricular function with conventional magnetic resonance imaging and echocardiography. Am J Cardiol. Jan; 2001 87(1):95–99. [PubMed: 11137841]
7. Nayak KS, Hu B. The future of real-time cardiac magnetic resonance imaging. Curr Cardiol Rep. Jan; 2005 7(1):45–51. [PubMed: 15610648]
8. Pennell DJ, Sechtem UP, Higgins CB, Manning WJ, Pohost GM, Rademakers FE, van Rossum AC, Shaw LJ, Yucel EK. Clinical indications for cardiovascular magnetic resonance (CMR): Consensus panel report. Eur Heart J. Nov; 2004 25(21):1940–1965. [PubMed: 15522474]
9. Ying L, Liang ZP. Parallel MRI using phased array coils. IEEE Signal Process Mag. Jul; 2010 27(4):90–98.
10. Candès EJ, Romberg J, Tao T. Robust uncertainty principles: Exact signal reconstruction from highly incomplete frequency information. IEEE Trans Inf Theory. Feb.2006 52:489–509.
11. Donoho DL. Compressed sensing. IEEE Trans Inf Theory. Apr.2006 52:1289–1306.
12. Candès EJ, Romberg JK, Tao T. Stable signal recovery from incomplete and inaccurate measurements. Comm Pure Appl Math. Aug; 2006 59(8):1207–1223.
13. Lustig M, Santos JM, Donoho DL, Pauly JM. k-t SPARSE: High frame rate dynamic MRI exploiting spatio-temporal sparsity. Proc Int Soc Magn Reson Med. 2006:2420.
14. Lustig M, Donoho D, Pauly JM. Sparse MRI: The application of compressed sensing for rapid MR imaging. Magn Reson Med. Dec; 2007 58(6):1182–1195. [PubMed: 17969013]
15. Jung H, Sung K, Nayak KS, Kim EY, Ye JC. k-t FOCUSS: A general compressed sensing framework for high resolution dynamic MRI. Magn Reson Med. Jan; 2009 61(1):103–116. [PubMed: 19097216]
16. Liang Z-P. Spatiotemporal imaging with partially separable functions. Proc IEEE Int Symp Biomed Imaging. 2007:988–991.
17. Candès EJ, Recht B. Exact matrix completion via convex optimization. Found Comput Math. Dec; 2009 9(6):717–772.
18. Haldar JP, Liang Z-P. Spatiotemporal imaging with partially separable functions: A matrix recovery approach. Proc IEEE Int Symp Biomed Imaging. 2010:716–719.
19. Zhao B, Haldar JP, Liang Z-P. PSF model-based reconstruction with sparsity constraint: Algorithm and application to real-time cardiac MRI. Conf Proc IEEE Eng Med Biol Soc. 2010:3390–3393. [PubMed: 21097243]
20. Jerosch-Herold M, Seethamraju RT, Swingen CM, Wilke NM, Stillman AE. Analysis of myocardial perfusion MRI. J Magn Reson Imaging. Jun; 2004 19(6):758–770. [PubMed: 15170782]

21. Wu YJL, Ye Q, Foley LM, Hitchens TK, Sato K, Williams JB, Ho C. In situ labeling of immune cells with iron oxide particles: An approach to detect organ rejection by cellular MRI. Proc Natl Acad Sci USA. Feb; 2006 103(6):1852–1857. [PubMed: 16443687]

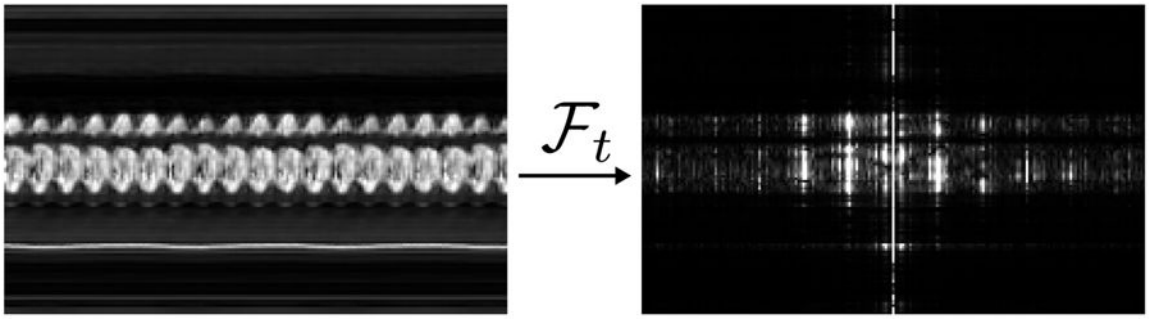


**Fig. 1.**
An illustration of spatial-spectral sparsity. *Left*, a spatial-temporal slice of a typical cardiac image function, and *right*, its corresponding spatial-spectral representation. The image in the spatial-spectral domain is highly sparse (or highly compressible).

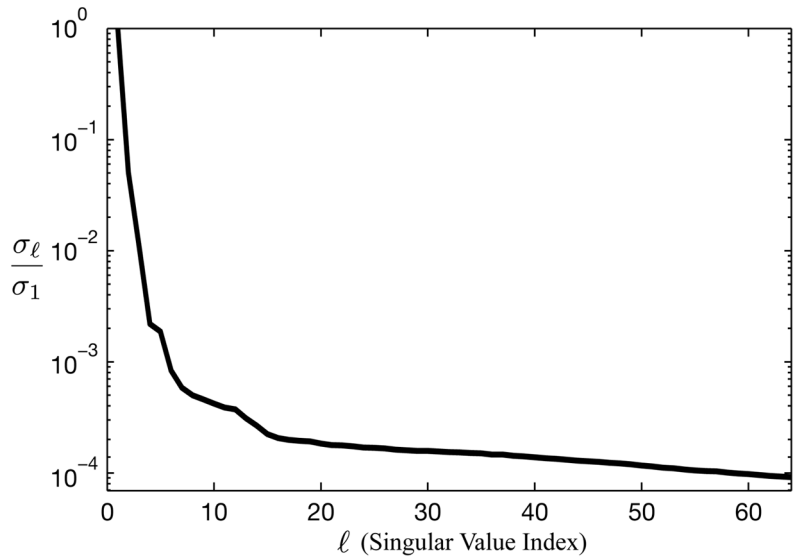


**Fig. 2.**

Plot of the normalized singular values (denoted by $\sigma$) of the Casorati matrix of a typical cardiac dataset. As can be seen, the singular values decay very quickly, resulting in an effective rank of about $L = 16$.

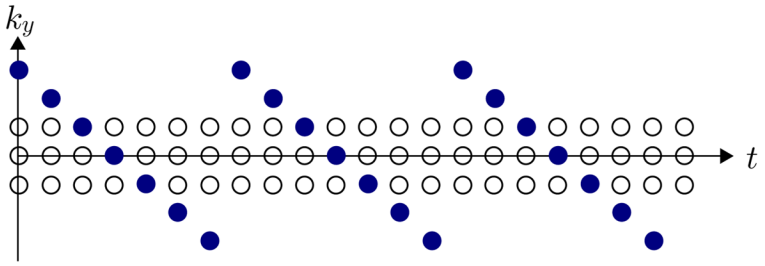


**Fig. 3.**

An example strategy to sparsely sample (**k**, *t*)-space. Note that the data acquired at the (**k**, *t*)-space locations marked by filled circles has limited **k**-space coverage but high temporal resolution, while the data at the (**k**, *t*)-space locations marked by outlined circles has extended **k**-space coverage and poor temporal resolution. These two datasets enable efficient determination of the PS model for the proposed method.

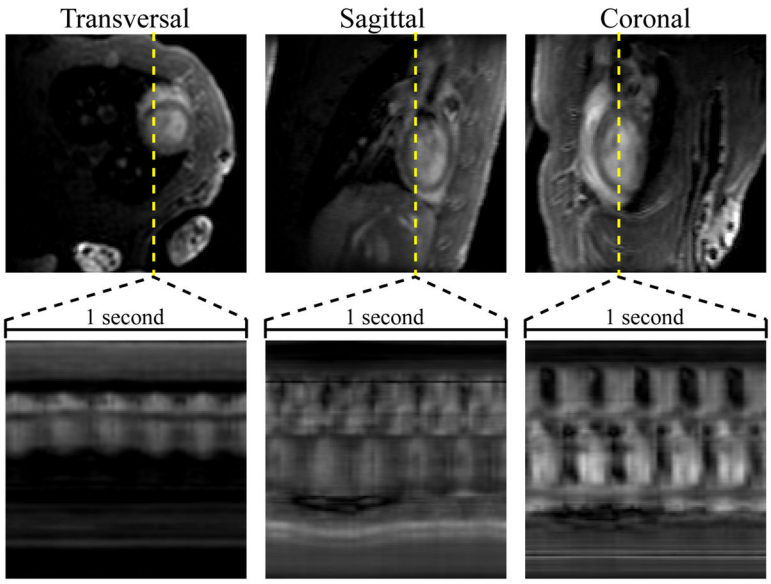


**Fig. 4.**

A subset of the reconstructed 4D image sequence depicting cardiac structure over one respiratory cycle. These images are appropriate for measurement of ejection fraction, cardiac output, as well as various other cardiac assessments.

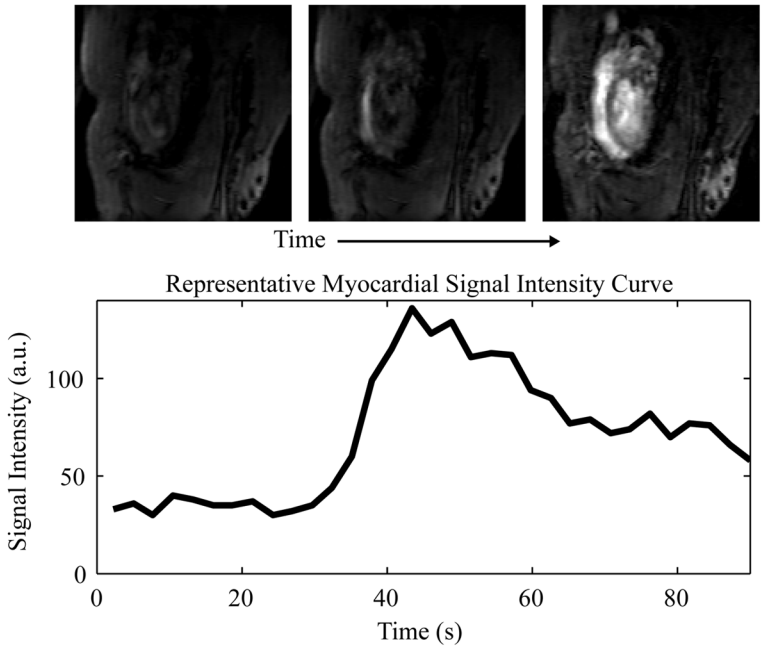


**Fig. 5.**

A subset of the reconstructed 4D image sequence depicting dynamic contrast enhancement for first-pass myocardial perfusion imaging. The images here show the wash-in of contrast agent. The signal intensity curve from a representative myocardial region is also pictured here; this curve may be used to measure myocardial blood flow or yield similar assessments of myocardial perfusion.